

To be submitted to
Nuclear Physics B

CERN/D.Ph.II/PHYS 74-9
16.4.1974

MULTIPLICITY CROSS SECTIONS FOR 100 GeV/c π^-p INTERACTIONS

E.L. BERGER^{*}, V.T. COCCONI, M.J. COUNIHAN^{**}, T. COGHEN^{***}, V. KARIMAKI⁺,
G. KELLNER, W. KITTEL⁺⁺, A. KOTANSKI⁺⁺⁺, D. KUHN^o, D.R.O. MORRISON,
P. SCHMID^{oo}, D. SOTIRIOU^{ooo}, R. STROYNOWSKI, F.A. TRIANTIS and H. WAHL.

CERN, Geneva

ABSTRACT

Charged particle multiplicity cross sections for 100 GeV/c π^-p inelastic interactions are presented and compared with results at other energies. The results for multiplicities $n \geq 4$ show a consistent trend in their energy dependence. The two prong cross section curve differs as it tends to flatten off at the higher energies. The zero-prong cross section values decrease steeply as $p_{lab}^{-1.1}$. The results for $n \geq 2$ for π^-p and pp reactions appear to lie on a "universal" curve if $(n \cdot \sigma_n / \sigma_{inel})$ is plotted against $\langle n \rangle / n$. This "scaling" rule is equivalent to KNO scaling, but the plot suggested here is more useful in studying low multiplicities. An interpretation in terms of a two component model and a possible extrapolation to higher energies are proposed.

* Visiting Scientist from Argonne Nat. Laboratory.

** CERN Fellow from Imperial College, London.

*** Now at Institute of Nuclear Physics, Cracow.

+ Now at the Department of Nuclear Physics, University of Helsinki.

++ Now at the University of Nijmegen, Physics Department.

+++ On leave from Jagellonian University, Cracow.

o CERN Fellow from Physikalisches Institut der Universität, Innsbruck.

oo CERN Fellow from Institut für Hoehenenergiephysik, Vienna.

ooo Now at Imperial College, London and CERN, NP-Division.

1. INTRODUCTION

Cross sections for production of a fixed number of charged particles are presented for π^-p inelastic interactions at 100 GeV/c, based on scanning twice approximately 50 000 photographs taken in the 30"-hydrogen bubble chamber at the National Accelerator Laboratory. These photographs, with an average of about 5 beam-tracks and 0.2 events per picture, yielded a total of 10 389 events. The calculation of the cross sections is described in sect. 2.

In sect. 3 our results are described and compared with the cross sections reported at other energies. In sect. 4 the physical significance of the results is discussed and in particular the energy dependence of the prong cross sections is interpreted in terms of a two component model. Speculations are made of possible behaviour at higher energies in sect. 5.

2. CALCULATION OF CROSS SECTIONS

To obtain the charged multiplicity cross sections, the following corrections have been made to the raw data obtained from scanning.

- i) Events of uncertain topology: 40 events were found whose topology could not be definitely decided, and were assigned to the topologies thought in the scannings to be most probably correct. Furthermore, 27 events appeared to have a missing positive track (20 three-prongs, 5 five-prongs, 1 seven-prong and 1 nine-prong). These were assumed to have a short recoil proton and were assigned to the next highest topology.
- ii) Secondary interactions: On 3.5% of secondary tracks, a secondary interaction is seen to occur in the bubble chamber, this proportion being almost independent of the number of tracks produced at the primary vertex. The mean charged multiplicity from secondary interactions is 2.9. Assuming a flat distribution of the distance of a secondary interaction from the primary vertex, and a "cut-off distance" of 0.5 cm below which a

secondary interaction cannot be clearly distinguished from the primary event, it is estimated that 52 events should have ambiguous topologies because of secondary interactions; 48 such events were found on scanning. Therefore, no further correction was applied and these 48 events were assigned to the next lowest topology.

- iii) V^0 's and γ 's close to the vertex: From the distribution of distances between the primary vertices and the observed V^0 's and γ 's, no evidence is found for any bias in prong-number counts caused by V^0 's close to the primary vertex; for the γ 's, a small correction is necessary amounting to a decrease by 0.015 in the mean charged multiplicity.
- iv) Scanning efficiencies: A small adjustment has been made to the number of two-prong events found on scanning because the scanning efficiency obtained from the comparison of the two scans was found to be 99.0%. For higher topologies, the scanning efficiency is very close to 100% and no corrections were applied.
- v) Dalitz pairs: To correct the data for the effect of Dalitz pairs which are not recognised as such, we first estimate the mean number of π^0 's produced per event. Assuming that $\langle n_{\pi^0} \rangle = \langle n_{\pi^+} \rangle = \langle n_{\pi^-} \rangle - \langle n_p \rangle$ and that $\langle n_{K^0} \rangle = \langle n_{\bar{K}^0} \rangle = \langle n_{K^-} \rangle = \langle n_{K^+} \rangle$, and incorporating our measurements of the mean numbers of V^0 decays and γ -conversions seen to occur in the bubble chamber, we find that $\langle n(\pi^0) \rangle = 2.6 \pm 0.1$. This would correspond to 400 Dalitz pairs in this experiment. The number of Dalitz pairs actually seen is 147 and so a correction is applied to the data on account of the unobserved 253; these were distributed among the various topologies in the same way as the 147 observed Dalitz pairs.
- vi) Elastic scattering: In the case of two-prong events, a correction for elastic scatters missed in both scans has to be made before the inelastic two-prong cross section can be obtained. These are the events that are not seen because of a very short recoil proton. Their number was estimated to be $15 \pm 5\%$ of the

elastic events seen^(*). This was obtained assuming that the effective minimum range of the recoil proton is 4 mm, that the exponential slope of the $d\sigma/dt$ distribution for elastic scattering is 10 GeV^{-2} and that the total elastic cross section at 100 GeV/c is $3.15 \pm 0.3 \text{ mb}$ (from interpolation of measured values [1-2]). The error on the elastic cross section is the main source of error in the inelastic two-prong cross section.

After applying corrections (i) to (vi), we have normalised the cross sections to the π^-p total cross section at 100 GeV/c taken to be $24.1 \pm 0.5 \text{ mb}$. This value was obtained by extrapolating the fit of the CERN/HERA Group [4] to the energy dependence of the π^-p total cross section in the range 20-60 GeV/c.

Table 1 shows the results obtained for the charged multiplicity cross sections. The errors given are dominantly statistical, but contain also appropriate allowance for the uncertainties inherent in all the corrections which have been applied to the data. They do not, however, contain the systematic error of about $\pm 2\%$ arising from their normalization to the estimated total cross section. The inelastic two prong cross section was obtained from the total two-prong cross section by subtracting the elastic contribution.

3. RESULTS AND COMPARISON WITH OTHER ENERGIES

From the cross sections for each charged multiplicity given in table 1, an average multiplicity $\langle n \rangle = 6.79 \pm 0.08$ and a dispersion $D = 3.16 \pm 0.04$ are calculated. In table 2 these and other parameters of the multiplicity distribution are summarised and their definitions given.

In fig. 1a the average multiplicity $\langle n \rangle$ is plotted against the square of the c.m. energy, s . Fitting the π^-p points [2,5] with the function $\langle n \rangle = a + b \log s/s_0$, with $s_0 = 1 \text{ GeV}^2$, one obtains $a = -0.56 \pm 0.09$ and $b = 1.40 \pm 0.02$, with $\chi^2/N = 3.1$, which corresponds to a 2% probability. The distribution of the π^-p points is not inconsistent with an increasing

(*) This estimate is in agreement with the results found in other high-energy experiments in this bubble chamber [2,3].

slope at the higher energies, which would indicate dominance of different effects in different energy ranges [6]. If one considers only the three points at 50, 100 and 200 GeV/c, the fit yields $a = -1.3 \pm 0.3$ and $b = 1.55 \pm 0.07$ with $\chi^2/N = 0.8$, corresponding to a probability of 37%.

A similar fit to pp data in the energy range 50-400 GeV/c gives $a = -2.9 \pm 0.3$ and $b = 1.80 \pm 0.1$ [7].

The correlation moment of the multiplicity distribution, f_2 , at 100 GeV/c is positive when all charged particles are considered and, as shown in fig. 1b, f_2 as a function of p_{lab} appears to cross zero somewhere between 30 and 70 GeV/c. On the other hand, when only negative tracks are taken, the value of f_2 is still negative at 100 GeV/c. From comparison with other energy points (not shown), our normalised central moments, γ_2 and γ_3 , are consistent with energy independence for $p_{lab} > 50$ GeV/c, as has already been found for pp data [8].

In fig. 2 the cross sections for each charged multiplicity are plotted as functions of the incident beam momentum for inelastic π^-p interactions from 2 to 200 GeV/c. The lines are hand-drawn for all multiplicities except for zero-prongs, as discussed below.

Considering multiplicities of 4 or more, the energy dependence of cross sections exhibit a consistent behaviour, as has already been observed in pp reactions. There is a steep rise from threshold, then a slower rise which for the lowest multiplicities, 4 and 6 prongs, is followed by a maximum and a decrease. The inelastic 2-prong cross section is already decreasing at 2 GeV/c and continues to do so at higher energies; in addition a further feature can be seen, namely the cross section flattens off above about 20 to 30 GeV/c. The zero-prong cross section is entirely different, as it presents a continuous decrease with increasing energy with no indication of any flattening off. It has been found that the zero-prong data can be fitted (5% probability) with the relationship

$$\sigma \sim p_{lab}^{-\alpha}$$

with a value of the exponent $\alpha = 1.07 \pm 0.03$.

The consistent trend of the multiplicity cross sections, apart from the zero-prong and possibly the 2-prong, suggests that some scaling relation may exist. An attempt^(*) to find such a scaling relation is shown in fig. 3. Here the prong cross section σ_n normalised to the total inelastic cross section, σ_{inel} , and multiplied by the charged multiplicity n , is plotted against the average charged multiplicity, $\langle n \rangle$, divided by n . This plot is shown in fig. 3a for π^-p reactions at 50, 100 and 200 GeV/c [2,5] and in fig. 3b for pp reactions at 50 to 400 GeV/c [3,10] for $n \geq 2$. It may be seen that the points which were well separated in fig. 1 now cluster about a single curve in fig. 3a, and similarly for pp reactions. Thus there is, in first approximation, good evidence that the quantity $n \cdot (\sigma_n / \sigma_{inel})$ is a function of $\langle n \rangle / n$ only, i.e.

$$n \cdot \frac{\sigma_n}{\sigma_{inel}} = \phi \left(\frac{\langle n \rangle}{n} \right) . \quad (1)$$

In terms of absolute value, the outstanding feature is an overall similarity between fig. 3a and 3b. This comparison of the plot of $n \cdot (\sigma_n / \sigma_{inel})$ against $\langle n \rangle / n$ for π^-p and pp is shown in fig. 4, where values for π^+p are also added [5]. The data are for incident momenta in the range 50 to 400 GeV/c. The general trend is the same for all three reactions although there are some small differences.

For multiplicities of 4 or more, the data points for different multiplicities have some overlap and the use of the word "scaling" is fully justified. For two prongs, however, the data points for this choice of energies, 50 to 400 GeV/c, do not overlap with other multiplicities, these points all having $\langle n \rangle / n$ values greater than 2.5. Thus for two prongs, the scaling is justified not by overlap for different multiplicities, but by the continuity of the trend of the results for $n \geq 4$ with those for $n = 2$ ^(**). Further work on low prong cross sections at higher energies is desirable.

(*) The original motivation for the choice of functions to be plotted was from a suggestion by Counihan [9] that the peak value of the n -prong cross section is proportional to $1/n$ and occurs at an energy characterised by a mean multiplicity $\langle n \rangle \approx n$. In fact, it may be seen from fig. 3 that if one takes $\sigma_{inel} \approx$ constant, then σ_n has a maximum when $\langle n \rangle \approx 0.8 n$, for each n .

(**) When low momenta (11 to < 50 GeV/c) data are plotted in fig. 4, the points lie close to the curve defined by the higher momenta data and in particular the 2-prong points are near the 4 prong values.

The scaling formula (1) proposed is basically equivalent to that given by Koba, Nielsen and Olesen [11] which has the form

$$\lim_{s \rightarrow \infty} \langle n \rangle \cdot \frac{\sigma_n}{\sigma_{inel}} = \Psi \left(\frac{n}{\langle n \rangle} \right) . \quad (2)$$

However, the method of plotting as in fig. 3 is particularly suitable for studying the behaviour of the lower multiplicities where diffractive effects are important, as discussed in the next section. Fig. 3 is essentially a plot of σ_n against energy, whereas KNO is essentially a plot of σ_n against multiplicity.

4. INTERPRETATION IN TERMS OF A TWO-COMPONENT MODEL

We now discuss these results in terms of a two-component model of high energy interactions. One component is diffractive and has a slow variation of cross section with energy, while the other is non-diffractive (e.g. a multiperipheral type mechanism) and has a cross section relatively rapidly decreasing with increasing energy for fixed n . The zero-prong channel cannot contain any diffractive reaction, and hence its cross section is expected to decrease steadily and rapidly with energy, and this is observed in fig. 2. On the other hand the two-prong inelastic cross section is expected to contain a contribution from non-diffractive processes, as well as a contribution from diffractive processes (e.g. $\pi^- p \rightarrow \pi^- (N\pi)^+$ and $\pi^- p \rightarrow pA_1 \rightarrow p(\pi^- \pi^0 \pi^0)$). The net result will then be that as the energy increases the 2-prong cross section will decrease at first rapidly, but then will flatten off as the diffractive channels become dominant. The asymptotic level of σ_n for 2-prongs is less than two millibarns.

5. POSSIBLE EXTRAPOLATION TO HIGHER ENERGIES

Results from NAL and the ISR [12] suggest that as the energy increases the multiplicity distributions of both diffractive and non-diffractive processes extend to higher and higher values of n . It is expected that the behaviour observed for the 2-prong cross section at presently available energies, viz. its flattening off, will also take place for higher multiplicities as higher energies are attained. That is, for each multiplicity one may expect

CERN/D.Ph.II/PHYS 74-9

the cross section to rise steeply above threshold, have a maximum, decrease fairly rapidly at first, then flatten off. The manner in which the cross section rises and achieves its maximum appears to be described by the "scaling" function shown in fig. 3. It will be of considerable interest to see whether the curves for higher multiplicities will flatten off and fall on the scaling curve defined now by the 2-prong data.

We are deeply indebted to the operating crews of the NAL accelerator and of the 30-inch bubble chamber. We would like to thank our scanning staff.

REFERENCES

- [1] Yu.M. Antipov et al., Nucl. Phys. B57 (1973) 333.
- [2] D. Bogert et al., π^-p Interactions at 200 GeV/c, NAL-Conf.-73/30-EXP.
- [3] J.W. Chapman et al., Phys. Rev. Letters 29 (1972) 1686.
G. Charlton et al., Phys. Rev. Letters 29 (1972) 515.
F.T. Dao et al., Phys. Rev. Letters 29 (1972) 1627.
C. Bromberg et al., Cross sections and Charged Particle Multiplicities at 102 and 405 GeV/c, UMBC 73-18 and UR-459.
- [4] E. Bracci et al., Compilation of Cross sections I - π^- and π^+ Induced Reactions, CERN/HERA 72-1.
- [5] See G.A. Akopdjanov et al., and the bibliography of $\pi^\pm p$ data given therein, to be published in Nuclear Phys. and CERN/D.Ph.II/74-4.
- [6] E.L. Berger and A. Krzywicki, Phys. Letters 36B (1971) 380.
- [7] T. Ferbel, Rochester preprint COO-3065-61 (1973).
- [8] Z. Koba and D. Weingarten, Lett. al. Nuovo Cimento 8 (1973) 303.
- [9] M.J. Coughlan, Some Consequences of the KNO Scaling Law for Charged Multiplicity Distributions, CERN/D.Ph.II/PHYS 73-45 (1973).
- [10] V.V. Ammosov et al., Phys. Letters B42 (1972) 519.
- [11] Z. Koba et al., Nucl. Physics B40 (1972) 317.
- [12] See e.g. D.R.O. Morrison, Fifth Hawaii Topical Conference, Aug. 1973, and CERN/D.Ph.II/PHYS 73-46.

TABLE 1

Prong number	No. of events found	Corrected No. of events	Cross section (millibarns)
0	16	16 ± 5	0.036 ± 0.011
2 total	1995	$2036 \pm 48^{\text{a)}}$	$5.10 \pm 0.4^{\text{b)}}$
2 inelastic	-	-	$1.95 \pm 0.29^{\text{c)}}$
4	2083	2108 ± 47	4.79 ± 0.11
6	2251	2276 ± 51	5.17 ± 0.12
8	1911	1892 ± 48	4.30 ± 0.11
10	1126	1102 ± 39	2.50 ± 0.09
12	625	622 ± 31	1.41 ± 0.07
14	278	264 ± 19	0.60 ± 0.04
16	70	59 ± 11	0.133 ± 0.025
18	23	20 ± 6.3	0.045 ± 0.014
20	7	6 ± 3.5	0.014 ± 0.008
22	4	3 ± 2	0.008 ± 0.0045
TOTAL	10389	10406	$20.95^{\text{d)}}$

Footnotes and caption for TABLE 1 :

- a) Without correction for elastic events.
- b) Corrected for elastic scattering as described in text.
- c) Assuming elastic cross section of 3.15 ± 0.3 mb as described in text.
- d) Total inelastic cross section (input datum, see text).

Table 1 : Number of events and cross section for each topology.

In addition to the errors given, the cross sections are subject to a systematic error of $\pm 2.1\%$ from their normalisation.

TABLE 2

Moments of the Multiplicity Distribution		
Quantity	all charged particles	Negatives only
$\langle n \rangle$	6.79 ± 0.08	3.39 ± 0.04
$D = [\langle (n - \langle n \rangle)^2 \rangle]^{\frac{1}{2}}$	3.16 ± 0.04	1.58 ± 0.02
$\langle n \rangle / D$	2.15 ± 0.04	2.15 ± 0.04
$\langle n(n-1) \rangle$	49 ± 1	10.6 ± 0.2
$f_2 = \langle n(n-1) \rangle - \langle n \rangle^2$	3.2 ± 0.3	-0.89 ± 0.09
$f_3 = \langle n(n-1)(n-2) \rangle - 3 \langle n(n-1) \rangle \langle n \rangle + 2 \langle n \rangle^3$	3.3 ± 1.2	1.7 ± 0.2
$\gamma_2 = \frac{\langle (n - \langle n \rangle)^2 \rangle}{\langle n \rangle^2}$	0.22 ± 0.01	0.22 ± 0.01
$\gamma_3 = \frac{\langle (n - \langle n \rangle)^3 \rangle}{\langle n \rangle^3}$	0.63 ± 0.01	0.63 ± 0.01

FIGURE CAPTIONS

Fig. 1 a) Average charged multiplicity, $\langle n \rangle$ and b) values of $f_2 = \langle n(n-1) \rangle - \langle n \rangle^2$, as functions of the square of the c.m. total energy, s , for $\pi^- p$ interactions [2,5].

Fig. 2 Charged multiplicity cross sections in $\pi^- p$ interactions as functions of the incident beam momentum [2,5]. The line through the zero-prong values is a fit to $\sigma_0 \sim p_{lab}^{-\alpha}$ with $\alpha = 1.07$. The other lines are drawn to guide the eye.

Fig. 3 "Scaling" plot of the energy dependence of the charged multiplicity cross sections, viz., $n \cdot (\sigma_n / \sigma_{inel})$ against $\langle n \rangle / n$ for a) $\pi^- p$ interactions between 50 and 200 GeV/c [2,5], b) pp interactions between 50 and 400 GeV/c [3,10].

Fig. 4 Plot of $n \cdot (\sigma_n / \sigma_{inel})$ against $\langle n \rangle / n$ for $\pi^- p$ [2,5], pp [3,10] and $\pi^+ p$ [5] interactions.

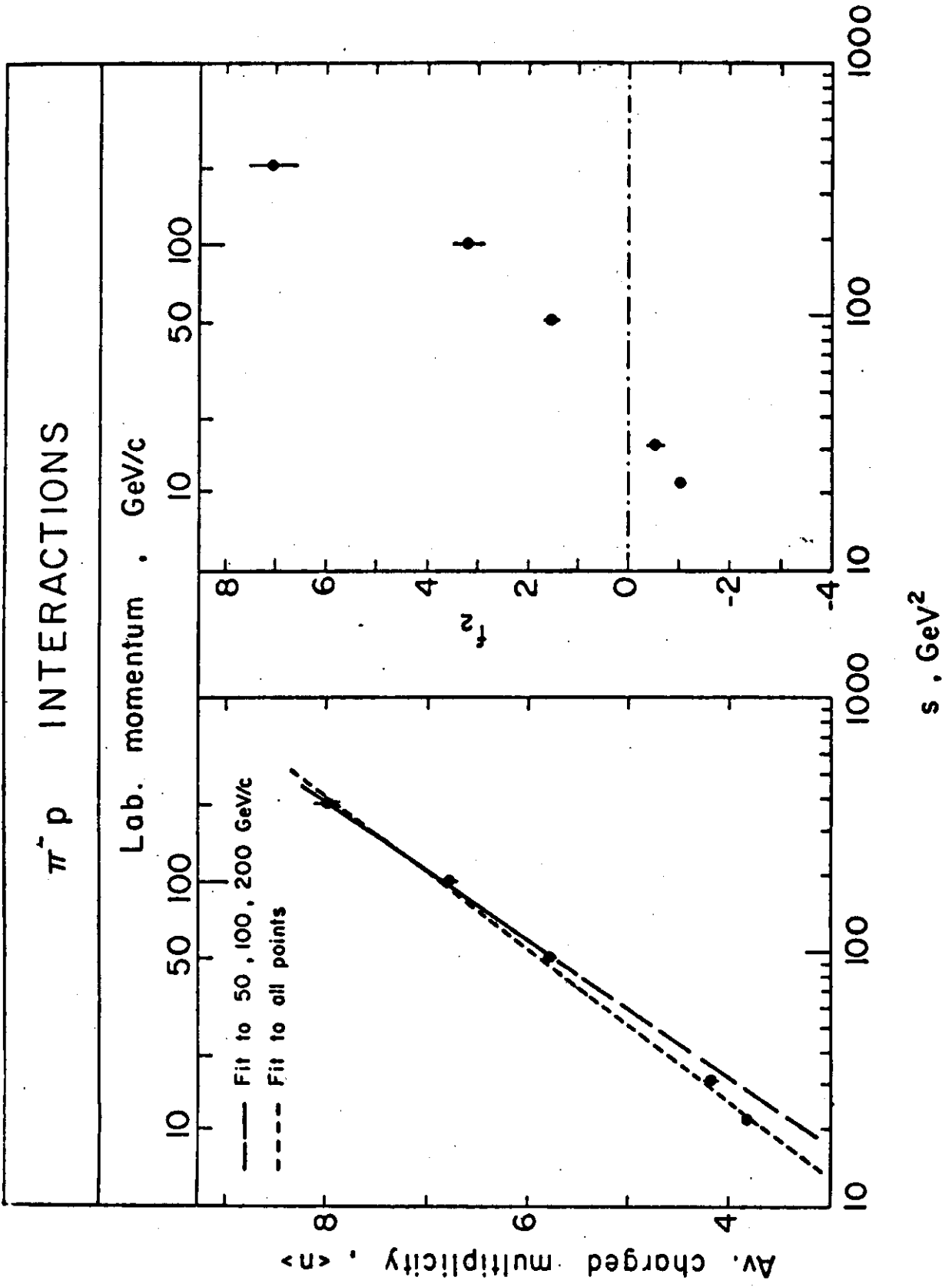


Fig. 1

Fig. 3

